Satellite-Based Water Depth Estimation: A Review

Kaixiang Wen[1,2], Yong Li[1,2(✉)], Hua Wang[1], Wenlong Jing[2], Ji Yang[2], Chen Zhang[2], and Zhou Wang[3]

[1] Guangdong University of Technology, Guangzhou 510070, China
5952546@qq.com
[2] Key Lab of Guangdong for Utilization of Remote Sensing and Geographical Information System, Guangdong Open Laboratory of Geospatial Information Technology and Application, Guangzhou Institute of Geography, Guangzhou 510070, China
[3] State Grid Panzhihua Power Supply Company, Panzhihua 617000, China

Abstract. This paper reviews the advances in water depth estimations from satellite images. According to the sensor type, current satellite-based water depth estimations are divided into two categories: optical-based and SAR-based (synthetic aperture radar) methods. By analyzing and discussing on the advantages and disadvantages of various methods. The following points can be summarized: First, the accuracy of optical remote sensing water depth detection method is higher than that of SAR-based models. Besides, optical-based method is simpler and less restricted than the SAR-based methods. Second, hyperspectral-based approach performed better than the multispectral optical remote sensing approaches. Since hyperspectral images provide richer spectral information than multispectral, which significantly matter in the water depth detection. Third, remote sensing water depth detection method is the best way to obtain the underwater topographic features of the inaccessible waters. Finally, on the basis of summarizing the previous water depth estimation methods, the development prospects of shallow seawater deep inversion technology are discussed and analyzed. For example, the establishment of an inversion model by fusing multiple remote sensing data, and the use of artificial intelligence technology for water depth inversion.

Keywords: Water depth inversion · Synthetic aperture radar · Hyperspectral · Multispectral remote sensing

1 Introduction

The water depth data is an important factor for obtaining and sensing the underwater topography. It is also an important project construction reference data for the development of the coastal marine economy [1, 2]. Traditional methods for measuring water depth include sounding rods, sounding line hammers, sonar sounding, etc. [1–3]. Although the accuracy is high, manual intervention, repeated operations, and high measurement cost are not met. Especially in the water depth measurement of some disputed islands and reefs, is impossible to carry out by relying on traditional artificial

Y. Xie et al. (Eds.): GSES 2019/GeoAI 2019, CCIS 1228, pp. 177–195, 2020.
https://doi.org/10.1007/978-981-15-6106-1_14

measurements. The development of remote sensing technology has solved the problem of traditional sounding surveying in large-area, all-weather, low-cost, disputed sea areas [3, 4].

Satellite remote sensing technology has just emerged in the 1960s and remote sensing water depth inversion has attracted attention. With the increasing types of remote sensing satellite sensors, the model research of water depth inversion using remote sensing images has been increasingly enriched. Water depth inversion based on multispectral optical images is particularly prominent. including theoretical analytical methods, semi-theoretical semi-empirical methods, and statistical methods [3–5]. There are also water depth inversion methods based on hyperspectral imagery such as Artificial Neural Network (ANN), principal component analysis, Bierwirth algorithm, linear unmixing method, look-up table method and spectral differential statistical method [6–9]. In addition, marine satellites such as Synthetic Aperture Radar (SAR) technology also play an important role in shallow water depth detection, such as Wave Number Spectrum Balance Equation (WNSBE), direct water depth Method and Bathymetry Assessment System (BAS) [10, 11]. Throughout the development process of remote sensing water depth inversion. Water depth inversion methods can be roughly divided into two categories: optical remote sensing inversion and Synthetic Aperture Radar (SAR) inversion. But there are many types of optical remote sensing sensors, rich data sources, and simple inversion methods, so they are the main methods of remote sensing water depth inversion. Although SAR remote sensing can be free from cloud and weather conditions, it needs to consider the influence of wind direction, wind speed, ocean wave and underwater topography in the process of water depth inversion. Therefore, these factors limit the wide range of applications of SAR water depth inversion technology.

This article has compiled a large number of methods for water depth inversion. A systematic review of the current theories and methods of water depth inversion from two aspects: optical remote sensing and synthetic aperture radar (SAR) inversion. What's more, the development prospects of current remote sensing water depth inversion methods are analyzed and prospected.

2 Water Depth Inversion of Optical Remote Sensing Imagery

2.1 Water Depth Inversion Method of Multispectral Imagery

The principle of optical remote sensing for detecting water depth is mainly based on the ability of light to transmit to water, and the transmission ability of visible light is particularly prominent in many spectral bands. The smaller the attenuation coefficient of water to visible light, the better its penetration into water. The value of visible light attenuation coefficient determines the measurable depth of multi-spectral remote sensing in water detection. When remote sensing of water depth, electromagnetic waves must be through the atmosphere and water. Because the electromagnetic wave in the visible light band has the strongest atmospheric transmittance and the smallest water body attenuation. So, it is the main relying band in optical water depth remote sensing measurement [3, 12–14]. Optical remote sensing water depth inversion models

can be divided into: theoretical analytical models, semi-theoretical semi-empirical models and statistical models.

Theoretical Analytical Method. The theoretical analysis method establishes a mathematical expression based on the amplitude value received by the satellite sensor, the water body reflectance value and the water depth value. Obtain the water depth value by solving the expression. The more common one is the simplified classical radiation equation, which is based on the Two-Stream Approximation Model. The Two-Stream Approximation Model divides the water depth into two part at any depth D: Dup and Ddw, so that the radiance value can be divided into two values. The change of radiance value is estimated by studying the relationship between radiance values of different water depth. Therefore, the distribution of water depth can be obtained by the water depth variable D of the analysis process [3, 15–17].

Radiative transfer equation:

$$\frac{dL(D,\varphi,\theta)}{dD} = -KL(D,\varphi,\theta) + L_P(D,\varphi,\theta) \tag{1}$$

$dL(D,\varphi,\theta)$ is the plane radiance from the water surface D to the θ angle and φ azimuth angle of the propagation direction; $L(D,\varphi,\theta)$ is the stroke function, representing the scattering gain; KLD, φ, θ is the attenuation loss function.

Lyzenga et al. [18] simplified the radiative transfer equation using a two-layer flow approximation model and abandons the reflection effect in the water to obtain the mathematical expressions of water surface reflection and water depth D. The expression is as follows:

$$R' = \frac{R_b\sqrt{1-X^2}\cosh(KD) + (X-R_b)\sinh(KD)}{R_b\sqrt{1-X^2}\cosh(KD) + (1-XR_b)\sinh(KD)} \tag{2}$$

$\mathrm{X} = \frac{\beta_b}{\alpha+\beta_b}, \mathrm{K} = (\alpha^2 + 2\alpha\beta_b)^{\frac{1}{2}}$ is water body attenuation coefficient; R' is effective scattering of water; R_b is the bottom reflectance of the water body; α is absorption coefficient; β_b is backscatter coefficient of water; D is indicate the water depth value.

The theoretical analytical method mainly obtains the water depth value by solving the physical parameters of each water body through the radiation transfer equation. Zhongliang Ping [16] used MSS-4 photos in the Jiaozhou Bay to derive a physical model of shallow sea water depth inversion based on the relationship between sea water transmittance, backscatter coefficient, sea floor reflectance and sea surface reflectance. Qidong Chen et al. [19] He derived a physical model of shallow sea depth inversion based on the radiative transfer equation and the optical thickness of the water body. In addition, he also considered the effects of chlorophyll and suspended sediment. Their experiments were applied in the Feilaixia Reservoir area in Guangdong and achieved good inversion results. Although this method has higher versatility, the calculation process requires a lot of physical and optical parameters, which is cumbersome and difficult to obtain. Therefore, it has not been widely promoted in practical applications.

Semi-theoretical Semi-empirical Method. The theoretical basis of the semi-theoretical semi-empirical method is the radiation attenuation of light in water. It is a method to achieve water depth inversion based on a combination of theoretical models and empirical parameters. This method mainly includes single-band linear regression method, dual-band linear regression method, multi-band linear regression method and logarithmic conversion ratio [3, 15–17].

1. Single-band linear regression method

The basis of the single-band linear regression method is the basement reflection water depth inversion model. Polcyn et al. [20] and Tanis et al. [21, 22] first applied this method:

$$L_i = L_{i\infty} + C_i R_B(\gamma) e^{-k_i f Z} \tag{3}$$

L_i is the amount of radiation in the i-band recorded by the satellite sensor; C_i is the constant of solar irradiance, atmospheric transmittance, water surface transmittance, and water surface refraction; $L_{i\infty}$ is the amount of radiation in the deep-water area; f is the length of the water path.

Although the theoretical inversion accuracy is high, the model relies on the conditions that are difficult to satisfy in practical applications. Therefore, scholars have improved the model to a certain extent to make it more suitable for water depth inversion in different waters. A water depth inversion method based on water body backscatter, as proposed by Wei [23]:

$$\mathrm{D} = -\frac{1}{k}\ln(1 - (L_i - B)/C) \tag{4}$$

B, C is the coefficient of the equation. Determined by the water depth value D and the radiation value L_i.

Qing Hang et al. [24] used the single-band model to perform water depth inversion on the Dongjiang River channel in the Pearl River Delta region based on the Landsat TM3 and TM2 bands and obtain the river topographic map. Based on the single-band model, Shufang Tian et al. [25] used correlation analysis to make a quantitative analysis of water depth and established a remote sensing model of salt-lake water depth. Xiaolei Guo et al. [26] compared single-band, dual-band, and multi-band water depth inversion methods at Longwan Port on Hainan Island using WorldView-2 images. They concluded that although the single-band linear regression method is simple to calculate, has few parameters, and is easy to implement, the accuracy of the obtained water depth value is poor (see Table 1).

2. Dual-band linear regression method

The dual-band linear regression method is based on the single-band linear regression method. Its purpose is to weaken the influence of the water body attenuation coefficient and the absolute value of the water body bottom reflectivity in different water types and water body sediments. It can suppress errors caused by surface fluctuations, satellite scanning angles and solar elevation angles. The dual-band linear regression equation can be expressed as follow:

Table 1. Accuracy analysis of water depth inversion in linear regression model [26]

Linear regression model	R^2	Fitting formula	MAE/m	MRE (%)	RMSE/m
Single band	0.434	Z = −35.810 * (X_{B3}) + 218.361	2.20	88.46	2.66
Dual band ratio	0.669	Z = −56.552 * (X_{B3}/X_{B1}) + 256.246	2.05	69.74	2.43
Multi-band	0.611	Z = −7.404 * (X_{B3}) − 49.337 * (X_{B4}) + 12.113 * (X_{B5}) + 12.542 * (X_{B6}) + 198.585	2.15	58.17	2.55

Suppose there are any two bands that have a constant reflectivity on different substrates:

$$\frac{(R_{a1})^{c1}}{(R_{a2})^{c2}} = \frac{(R_{a1})^{c1}}{(R_{a2})^{c2}} = C \tag{5}$$

$$\mathrm{D} = \frac{w_1}{2K_1}(lnR_{b1} + lnk_1 - X_1) + \frac{w_2}{2k_2}(lnR_{b2} + lnk_2 - X_2) \tag{6}$$

$X_1 = \ln[R_{E1} - R_{W1}]; X_2 = \ln[R_{E2} - R_{W2}]; w_1$, w_2 is dual-band weighting factor.

When $w_1 = \frac{C_1K_1}{C_1K_1 + C_2K_2}, w_2 = \frac{-C_2K_2}{C_1K_1 + C_2K_2}, d = \frac{w_1}{2K_1}lnk_1 - \frac{w_2}{2K_2}lnk_2$, we can obtain the final water depth expression D:

$$\mathrm{D} = \mathrm{a}X_1 + bX_2 + c \tag{7}$$

Because the dual-band linear regression method can overcome the shortcomings of the single-band linear regression method, it is more widely used. Qingjiu Tian et al. [27] used the TM3 and TM4 bands, which are sensitive to water depth, to perform water depth inversion in the offshore waters of Jiangsu. The predictions obtained from their experiments fit well with the measured water depth. Dong Zhang et al. [28] used the TM4 or TM2 band to establish a linear regression relationship to perform water depth inversion in the Yangtze Estuary waters also obtained good results. Ming Chen et al. [29] performed the ratio processing on the TM2 and TM4 band. What's more, they made 16 sections at 1 km intervals according to the size of the study area. They

compared according to the water depth of each section and got a good result with an average agreement rate of 82%.

3. Multi-band linear regression method

The multi-band linear regression method is extended to N bands and the reflectivity of N different water bodies based on the dual-band linear regression method. John et al. [30] derived multi-band linear regression water depth inversion method based on e-exponential decay optical mode:

$$\mathrm{D} = a_1 X_1 + a_2 X_2 + \ldots + c \tag{8}$$

Multi-band comprehensive consideration of all aspects of water depth information has higher water depth inversion accuracy than single-band and dual-band. So it is more widely used. Clark et al. [31] used multi-band linear regression and Landsat4 imagery to perform water depth inversion on islands in the southeastern coast of Puerto Rico in the Caribbean. They obtained the root mean square error between the predicted water depth and the measured water depth is 1.86 m. Kaichang Di et al. [32] introduced piecewise linear regression and data normalization techniques to improve the multi-band linear regression method. Therefore, this method is more suitable for large-scale sea water depth inversion with improved accuracy. Dianyuan Xu [33] uses the image gray values of MSS4, 5, and 7 to establish a relationship with the measured water depth. Then, based on this relationship, the predicted water depth distribution is obtained and the Yellow River waters are interpreted.

4. Logarithmic conversion ratio method

When using the linear regression method for water depth inversion, the difference between the radiance value received by the satellite sensor and the radiance value in the deep water region may be negative. Therefore, it may not be used in complex sea areas with large range and low radiance value. For this reason, Stumpf et al. [34] proposed a log-transformation ratio method by correcting the linear model:

$$\mathrm{D} = m_1 \frac{\ln(nR_w(\lambda_i))}{\ln(nR_w(\lambda_j))} - m_0 \tag{9}$$

D is the water depth; m_1, n is a constant used to adjust the water depth ratio; m_0 is used to compensate for zero meter depth; $R_w(\lambda_i)$, $R_w(\lambda_j)$ is the reflectance of the corresponding band.

In the study of later water depth inversion, Zhen Tian [8] changed the adjustment factor of Stumpf model to two and compensated the water depth inversion results of different water bodies to some extent. And the inversion accuracy obtained by studying the waters around the East Island is higher than that of the Stumpf model. The improved model is as follows:

$$D = m_1 \frac{\ln(nR_w(\lambda_i))}{\ln(mR_w(\lambda_j))} + m_0 \tag{10}$$

Xiaolei Guo et al. [35] built a geo-adaptive model based on the log-ratio model to perform water depth inversion in the eight ports of Hainan. This model improves the problem of uneven substrate and water body in the global model inversion process. Therefore, the accuracy of water depth inversion can be improved and the error can be controlled within 1 m. Anna Chen et al. [36] based on GeoEye-1 multispectral imagery used log-linear models, log-transformation ratio models, and improved log-transformation ratio models to perform water depth inversion for Wuzhizhou Island and Penang. They concluded that the improved logarithmic conversion ratio model has the highest inversion accuracy and stability in different water quality and depth. but the logarithmic conversion ratio model is not good, while the logarithmic linear model is susceptible to seawater environment and not stable enough.

Statistical Methods. The statistical method is to obtain water depth data by analyzing the correlation between the gray value of the multispectral remote sensing image and the measured water depth value. Its mathematical expression is as follows:

$$D = f(X_1, X_2 \ldots X_n) \tag{11}$$

D is the water depth value; $X_i (i = 1, 2, \ldots n)$ is the band of the image.

Lyzenga et al. [18, 37] used principal component analysis to assume that the gray value of the image is linearly related to the water depth value:

$$X_i = ln(L_i - L_{si}) \tag{12}$$

Generate new variables Y_i by rotating the coordinate system on X_i;

$$Y_i = \sum_{j=1}^{N} A_{ij} X_j \tag{13}$$

If this is a pure rotation, then only Y_i is a variable related to water depth, and the other $i - 1$ variables are only related to the bottom reflectance; the water depth variable can be expressed as:

$$Y_N = B_m - C_z \tag{14}$$

B_m is the bottom composition function, C_z determined by the water attenuation coefficient. This method provides a more accurate water depth value by selecting the appropriate band in a clear ocean with a depth of no more than 15 m.

Artificial neural networks [38] is also a type of statistical method often used in water depth inversion. Because of its self-learning, self-organizing, adaptive and nonlinear dynamic processing, it has more powerful approximation ability than the traditional statistical method in simulating nonlinear change systems. The network of error reverse propagation algorithm, referred to as BP neural network [39]. It takes the

spectral characteristic value of the image as input and the water depth value as the desired output. The simplest structure is usually three layers of an input layer, an intermediate layer (hidden layer) and an output layer (see Fig. 1).

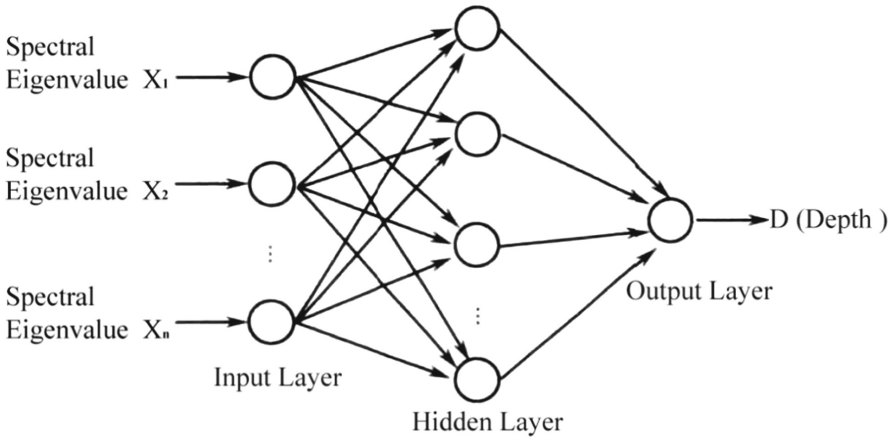

Fig. 1. Schematic diagram of BP neural network structure [40]

BP network algorithm weight formula is as follows:

$$\mathrm{E} = \frac{1}{2}\sum_{j=1}^{m}\left(Y_j - \hat{Y}_j\right)^2 \tag{15}$$

Y_j is the target value, $\hat{Y}_j$ is the expected output value, m is the number of neurons in the output layer.

$$w_{ij}(p+1) = w_{ij}(p) + \alpha\Delta w_{ij}(p+1) - \mu\frac{\vartheta E(p)}{\vartheta w_{ij}(p)} \tag{16}$$

α is the momentum coefficient μ is the learning coefficient and the range of values is between 0 and 1.

Although BP neural network has powerful computing power, it is easy to cause over-fitting, slow convergence and sensitivity to initial weight. What's more, it requires a large amount of known water depth data as a training sample, which limits its wide application. Bin Cao et al. [40] based on the traditional BP neural network algorithm and overcome its shortcomings proposed an improved algorithm for water depth inversion. Cao used this algorithm to experiment on Ganquan Island in Sansha, Hainan. The results show that the improved BP network algorithm has relatively high accuracy and fast convergence speed. Yanjiao Wang et al. [3] used 3 layers of BP neural network and 600 water depth samples as training samples to better invert the water depth of the Nangang section of the Yangtze River estuary, with an average absolute error of 0.9 m.

2.2 Water Depth Inversion Method of Hyperspectral

The resolution of hyperspectral spectrum reaches nm level, and the number of bands is several dozen more than that of multi-spectrum. Therefore, there are many advantages to using water depth detection in its image. Hyperspectral spectrum can provide multiple bands for band combination. What's more, Hyperspectral spectrum use its rich image band information to identifies waterborne sediments and water types, reducing the impact of other factors in water depth inversion [8].

The Artificial Neural Network Method. The mathematical model is the same as the BP neural network in the statistical method. Yingni Shi [9] uses the principal component analysis of the input variables and normalizes the peaks to improve the learning speed of the neural network. And then, perform water depth inversion experiments in the study area. They concluded that the water depth based on the inversion of hyperspectral image neural network algorithm is better than the semi-analytical model. Sandidge et al. [41] used the BP neural network algorithm to perform water depth inversion in the waters around Florida based on the correlation established between the hyperspectral image and the measured water depth. The results show that the artificial neural network predicts the water depth is consistent with the measured water depth, which is superior to the traditional statistical methods.

Semi-analytical Model Method. Hyperspectral Optimization Process Exemplar (HOPE) is the main method for current water depth inversion of hyperspectral remote sensing. The core of the algorithm is to establish the functional relationship between remote sensing image reflectivity, water body, water body sediment and water depth. This method was first proposed by Lee et al. [42, 43] and its expression is as follow:

$$R_{rs}(\lambda) = f[a(\lambda), b_b(\lambda), \rho(\lambda), H, \theta_\omega, \theta_v, \varphi] \tag{17}$$

$a(\lambda)$ is the water absorption coefficient; $b_b(\lambda)$ is the backscatter coefficient of water; $\rho(\lambda)$ is the water body reflectivity; H is the water depth; θ_ω is the lower surface solar zenith angle; θ_v is the lower surface nadir angle of view; φ is the field of view azimuth.

This model has introduced large number of water and physical parameters, so it's comprehensive calculation with small error has been widely used. Lee et al. [44] used this model algorithms and AVIRIS hyperspectral images to perform experiments in Tampa Bay, Florida has obtain better water depth inversion results. Mcintyre M L et al. [45] used a semi-analytical model and hyperspectral imagery for water depth inversion in the 10-15 m waters of Florida. Obtained the average deviation of the predicted water depth is 4.9% and the RMS is 7.83%. Lee et al. [45] Based on the water depth inversion model and use the NASA EO-1 hyperspectral image with a resolution of 30 m has obtained an average error of only 11% compared to LIDAR. Zhen Liu et al. [7] used the HOPE algorithm and semi-analytical model perform water depth and optical parameters inversion of the South Island reef. Their experiment obtained a good result. For other methods, Zhang et al. [46] used a lookup table approach to reverse the water depths of the waters around Peter Island in the Virgin Islands. Zhishen Liu [47] inverted the water

depth of the Smith Island Bay using Principal Component Analysis and obtained the error in the deep-water area is 1 m and the shallow water zone error is 0.2 m.

3 The Method of Synthetic Aperture Radar (SAR) Water Depth Inversion

3.1 The Principle of Synthetic Aperture Radar (SAR) Water Depth Inversion

The working band of SAR does not directly penetrate seawater to detect underwater terrain. It indirectly measures underwater terrain by receiving backscattering from the sea surface, because the undulations of the underwater terrain change the backscattering intensity of the sea surface as a change of bright and dark stripes on the radar image.

3.2 The Inversion Method Water Depth Estimation System

The water depth estimation system [11, 48] is currently a highly accurate algorithm for shallow seawater deep inversion using radar images. This algorithm was developed by the Dutch company ARGOSS. It consists of a SAR image simulation model and a data assimilation model. The schematic of the BAS system is as Fig. 2:

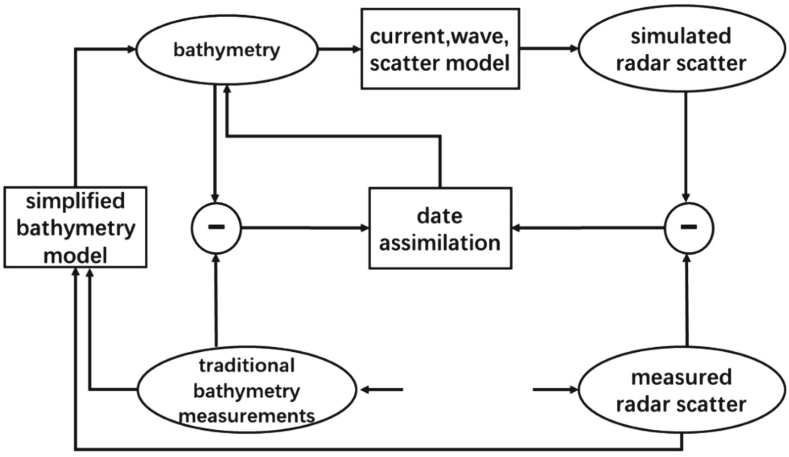

Fig. 2. BAS water depth estimation system [49]

Calkoen et al. [49–51] used the BAS technique to conduct a water depth estimation test at the tidal inlet between the small islands of Ameland and Schiermonnikoog in Waddenzee, northern Netherlands. The mean square error of water depth obtained by this work is 0.36 m. However, the shortcoming is that the method is more troublesome

to measure in shallow waters of 30 m and requires intensive measurement of water depth sampling spacing.

3.3 The Inversion Method of Direct Water Depth

Direct water depth inversion is based on the interaction of three models of radar underwater terrain imaging and reuse simulation model to obtain water depth data. Among them, the simulation model includes the Nevi-Stokes equation, the continuity equation, the spectral action balance equation, and the radar backscatter model [1, 2]. The specific calculation steps are as Fig. 3:

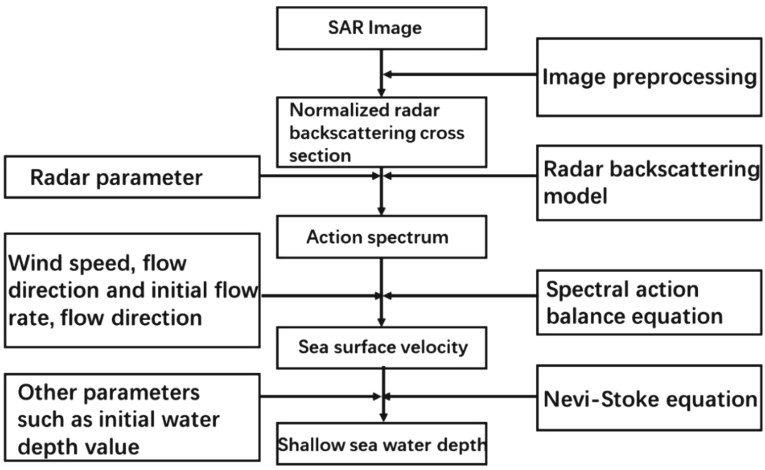

Fig. 3. Direct water depth inversion

$$\frac{\partial V_x}{\partial_t} + V_x\frac{\partial V_x}{\partial_x} + V_y\frac{\partial V_x}{\partial_y} - FV_y + g\frac{\partial \xi}{\partial_x} + g\frac{V_x\sqrt{V_x^2+V_y^2}}{c^2(h+\xi)} - \frac{\tau_x}{\rho(h+\xi)} = 0 \tag{18}$$

$$\frac{\partial V_y}{\partial_t} + V_x\frac{\partial V_y}{\partial_x} + V_y\frac{\partial V_y}{\partial_y} - FV_x + g\frac{\partial \xi}{\partial_y} + g\frac{V_y\sqrt{V_x^2+V_y^2}}{c^2(h+\xi)} - \frac{\tau_y}{\rho(h+\xi)} = 0 \tag{19}$$

$$\frac{\partial \xi}{\partial_t} + \frac{\partial[(h+\xi)V_x]}{\partial_x} + \frac{\partial\left[(h+\xi)V_y\right]}{\partial_y} = 0 \tag{20}$$

The above Eq. (18) is the Nevi-Stokes equation and the (19) continuity equation. V_x, V_y is the water flow velocity in the X and Y directions, ξ is the relative horizontal potential height, h. The distance between the bottom of the sea and the horizontal potential surface, F is the Coriolis parameter, c is XieCai parameter, τ_x, τ_y is the wind stress in

the X and Y directions, ρ is the wind stress in the X and Y directions, g is gravitational acceleration [1, 2, 10].

$$\frac{dA\left(\vec{r},\vec{k},t\right)}{d_t} = \left(\frac{\partial}{\partial_t} + \frac{d\vec{r}}{d_t}\frac{\partial}{\partial\vec{r}} + \frac{d\vec{k}}{d_t}\frac{\partial}{\partial\vec{k}}\right)A\left(\vec{r},\vec{k},t\right) = S_r\left(\vec{r},\vec{k},t\right) \tag{21}$$

The above formula (21) is the spectral action balance equation; $A\left(\vec{r},\vec{k},t\right)$ is the action spectrum, $\vec{r} = (x, y)$ representing spatial variables, $\vec{k}$ is the representative wave number, $S_r\left(\vec{r},\vec{k},t\right)$ is the original function representing the wave composition wave.

The radar backscattering model [1, 2, 11] has a two-scale model, Bragg model and Kirchoff scattering model. The two-scale model is mainly used for rough sea surfaces that cannot clearly distinguish the undulating scale. The kirchhoff scattering model is mainly used for large-scale undulating rough sea surface and the situation of 0°–20° satellite incident angle. However, The Bragg model is mainly used for small-scale undulating rough sea surface and the situation of 20°–70° satellite incident angle. Because the incident angle of spaceborne synthetic aperture radar is mostly 20°–70°, most researchers use this model as the radar backscattering model.

$$\sigma^0_{pq}(\theta) = 16\pi k^4 cos^4(\theta)\left|G_{pq}(\theta)\right|^2\varphi(k_B, 0) \tag{22}$$

p, q related to polarization, wave number, angle of incidence, and function $G_{pq}, k_B = 2ksin\theta$ is the Bragg wave number, G_{pq} function expression is as follow:

$$G_{HH}(\theta) = \frac{\varepsilon_r - 1}{\left(cos\theta + \sqrt{\varepsilon_r - sin^2\theta}\right)^2} \tag{23}$$

$$G_{VV}(\theta) = \frac{\varepsilon_r - 1[\varepsilon_r(1 + sin^2\theta) - sin^2\theta]}{\left(\varepsilon_r cos\theta + \sqrt{\varepsilon_r - sin^2\theta}\right)^2} \tag{24}$$

ε_r Representing the complex permittivity of seawater.

Bin Fu [1, 2] inversion of the Xiaoyinsha sea area in Keelung Island and Jiangsu offshore by direct inversion method. The root mean square error of the retrieved water depth value and chart water depth value in the Xiaoyinsha area is 0.42 m. Xiaolei Bi [52] used the direct inversion method to carry out the water depth test in the Taiwan Strait and classified according to radar polarization. Draw the best conclusion from the results of the full-polarization SAR inversion.

3.4 The Inversion Method of Wavenumber Spectrum Balance Equation (WSBE)

Based on the Bragg model, large-scale background flow field model, and two-dimensional shallow water dynamics equations, the steepest descent method is used to iteratively obtain the shallow sea depth [11]. The numerical model is as follows:

$$G(V_x, V_y, \theta_1) = cos^2\theta_1 \frac{\partial V_x}{\partial x} + cos\theta_1 sin\theta_1 \times \left(\frac{\partial V_x}{\partial y} + \frac{\partial V_y}{\partial x}\right) + \frac{\partial V_y}{\partial y} sin^2\theta_1 \tag{25}$$

(25) is a first-order approximate analytical expression of the gradation value of the SAR image; wherein, θ_1 is the sea surface wind direction.

$$\frac{\partial V_x}{\partial t} + V_x \frac{\partial V_x}{\partial x} + V \frac{\partial V_x}{\partial y} - fV_y = -g \frac{\partial \xi}{\partial x} + \frac{cV_x}{(h+\xi)} \tag{26}$$

$$\frac{\partial V_y}{\partial t} + V_x \frac{\partial V_y}{\partial x} + V \frac{\partial V_y}{\partial y} - fV_x = -g \frac{\partial \xi}{\partial y} + \frac{cV_y}{(h+\xi)} \tag{27}$$

$$\frac{\partial \xi}{\partial t} + \frac{\partial((h+\xi)V_x)}{\partial x} + \frac{\partial\left((h+\xi)V_y\right)}{\partial y} = 0 \tag{28}$$

(26) (27) (28) is the two-dimensional shallow hydrodynamic equation.

$$J(V_x, V_y, h, \xi) = \int_{D_0} \left(f_1^2 + f_2^2 + f_3^2 + f_4^2\right) dxdy \tag{29}$$

(29) is targeted function $J(V_x, V_y, h, \xi)$, wherein:

$$f_1 = \alpha_1 \left(-fV_x + g\xi_x + \frac{cV_x}{h+\xi} + V_x V_{xx} + V_x V_{xy} + V_{xt}\right) \tag{30}$$

$$f_2 = \alpha_2 \left(fV_x + g\xi_y + \frac{cV_x}{h+\xi} + V_y V_{yy} + V_x V_{xy} + V_{yt}\right) \tag{31}$$

$$f_3 = \alpha_3 \left[\left(l_m l_n + \frac{1}{2} l_\alpha l_\beta \xi_{\alpha\beta} L_m L_n\right) \frac{\partial u_m}{\partial x_n} - G\right] \tag{32}$$

$$f_4 = \alpha_4 \left(V_x(h+\xi)_x + V_y(h+\xi)_y + V_{xx}(h+\xi) + V_{yy}(h+\xi) + \xi_t\right) \tag{33}$$

Changshui Xia [53] used the wave number balance equation to invert the water depth in the Tanggu sea area. They found that the inversion water depth and the actual water depth are in good agreement. The average relative error of the two sections taken in the image is 8.9% and 9.2%, respectively. Jungang Yang et al. [54] used WNSBE technology and two ERS-2 images imaged at different time to invert the water depth near the Taiwan Strait. Experiments show that the smallest inversion error can reach 2.23 m (Fig. 4).

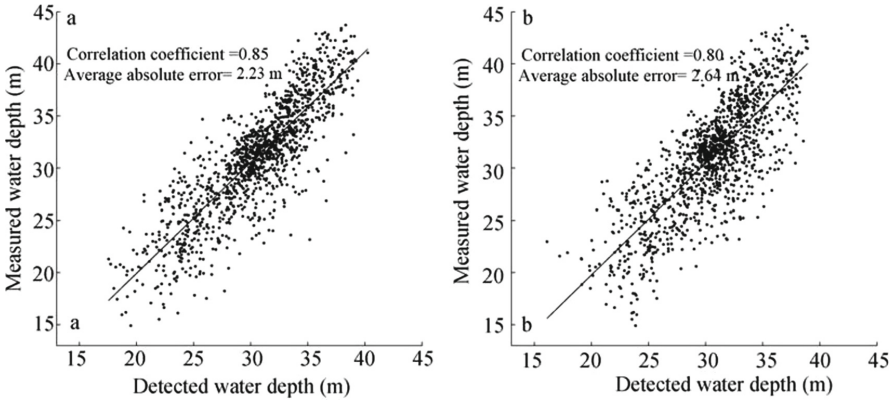

Fig. 4. Water depth inversion comparison chart [54]

Zejun Li et al. [55] improved the method on the basis of Jungang Yang scholars. He used this method and ERS-2 and ENVISAT data to conduct water depth inversion experiments to obtain ideal inversion results (Table 2):

Table 2. Water depth inversion results [55]

Name	Absolute variation error	Relative variation error
ERS-2 data	3.8 m (8.9%)	1.18 m (27%)
ENVISAT data	4.5 m (10.8%)	2.94 m (69%)

The method of retrieving the water depth based on the synthetic aperture radar image is not directly obtained water depth information on image. So, the water depth obtained by the interaction calculation of shallow sea topography, sea surface current, wind speed and the like. The BAS method requires more measured water depth information when calculating. The more accurate the water depth data is, the higher accuracy the experimental results will be. Submarine depth inversion is required in areas with complex underwater terrain or large height differences. Otherwise, the error is large. The direct water depth inversion method has higher requirements on the quality of SAR images. What's more, the image noise contributes a lot to the water depth error. The image gray scale simulation model of the wave number balance equation has higher requirements on wind direction. So, it's calculation of water depth is more complicated than the former two.

4 Prospect of Remote Sensing Water Depth Inversion Technology

The remote sensing water depth inversion technology has formed a relatively complete theoretical and practical basis from the 1960s to the present. This paper expounds the research results of remote sensing water depth inversion from the aspects of optical remote sensing and synthetic aperture radar remote sensing. Inductively analyze its advantages and disadvantages in order to present a rich and comprehensive review article for readers. As we all know, water depth inversion still has large uncertainties, such as remote sensing image deformation caused by atmospheric and topographical effects, low resolution of image, weak water permeability of water band, complex water reflection mechanism, and uncertainties in water body. Therefore, improving the accuracy of water depth inversion is a systematic problem. It is necessary to consider not only the optimization of inversion methods, but also the means of obtaining data and the method of improving data preprocessing.

From the previous review, we can see that the main problems of water depth inversion technology are as follows:

1. Remote sensing image preprocessing

Since the imaging process of satellites is affected by sensors, atmosphere and terrain. If we want to obtain a real image, it is necessary to perform atmospheric correction, geometric correction, and noise filtering on the original image. The image cannot be realistically restored in various pre-processing, and other errors may be introduced. For example, atmospheric correction processing needs to use different models for different remote sensing images to correct the effects of atmospheric molecules such as aerosols. In addition, the image resolution and the measured water depth are not an exact match relationship, which is a pixel value corresponding to a range of water depths. That is, the water depth data we actually measured is the precise water depth of a certain point. But the image such as a pixel of the Sentinel_2 green band corresponds to a range of 10 m $\times$ 10 m on land. What's more, for complex seabed topography, this range of water depth changes will be large, which undoubtedly affects the accuracy of water depth inversion.

2. Nautical water depth

Water depth inversion is mainly applied to uninhabited sea areas. So, the measured water depth often depends on the water depth data on the chart. The water depth data on the chart is the reference surface depth at a certain point, but the instantaneous water depth at a certain point is recorded during image imaging. Therefore, it is necessary to change the chart water depth to the synchronized instantaneous water depth based on the time of image formation and the tide data. This correction process will undoubtedly introduce errors and lead to low accuracy of later water depth inversion.

3. Water depth division

The water depth inversion technology is not only regional, but also has different water depth intervals. This is mainly because different wave bands penetrate water bodies at

different depths and carry different amounts of water depth information. Therefore, for the same inversion method, it is also necessary to perform inter-zone inversion of water depth to ensure better inversion results.

4. Water quality

Most of the water depth inversion are clear Class I water bodies. These water suspensions are less, not turbid, and have a homogeneous bottom material, so the water depth inversion is not suitable for all water bodies. If the water bodies is not clear, the sun's light waves will be reflected and scattered by the suspended sediment in the water after entering the water body, which weakens the emissivity of the water. On the other hand, if the water contains a lot of impurities such as chlorophyll and plankton, these impurities will also reflect and absorb sunlight. Only a small amount of light waves are absorbed and reflected by the water bottom and then captured by the receiver. However, if the substrate is not uniform, the reflected light wave will be further weakened. What's more, The weakly reflected light received by the receiver will also contain spectral information of impurities such as chlorophyll. If these problems are not dealt with in later water depth inversion models, this will cause large errors in experimental results.

5. Synthetic Aperture Radar Inversion Difficulties

Although Synthetic Aperture Radar has the advantage of being weather-free throughout the day, the inversion method is computationally intensive. This method is greatly affected by terrain slope, sea surface waves, and wind speed, so that its inversion accuracy is poor. This is why it is difficult to be widely used.

Nevertheless, the water depth inversion technology is still an important water depth detection technology for current sea chart sounding and marine engineering safety. With the launch of high-resolution satellites, hyperspectral satellites, and ocean sounding radars, researchers will explore more accurate water depth inversion techniques in this area, such as:

- Combined inversion of multiple data sources: Hyperspectral satellite data combined with Multi-spectral satellite data. Inversion of Airborne Lidar Data with Multispectral and Hyperspectral Data. Long-term sequence satellite data inversion. Synthetic Aperture Radar combined with Optical image inversion.
- Classification of water quality parameters: Classification of suspended sediment, chlorophyll, and bottom sediment in water. Then use it as an influence factor to establish a relevant model for water depth inversion.
- Water body inversion by area and depth by depth: Proper partitioning of a wide range of water bodies and then selecting a matching model for water depth inversion. So, we can get more accurate water depth data. Different depths of depth are also used for segmentation inversion. Selecting appropriate water depth inversion models for different water depths makes the fitting effect better and reduces the inversion error.
- Artificial intelligence technology water depth inversion: Autonomous training of large amounts of water depth data and remote sensing data using algorithms of machine learning and deep learning. Use its excellent computing power and fitting

accuracy to obtain accurate inversion water depth and achieve automatic inversion. Of course, this also needs to solve the problem of various data source fusion, time series problems [3, 14, 17].

Remote sensing water depth inversion has the advantages of low cost, large range and real-time. It complements traditional water depth measurement methods and has broad development prospects. If we can make a major breakthrough in data acquisition and inversion methods, there will be a wider range of practical applications.

Acknowledgments. This study was jointly supported by the National Natural Science Foundation of China (41976189, 41976190); Special Fund for Development of Guangdong Academy of Sciences (2019GDASYL-0502001); China Southern Power Grid Guangzhou Power Supply Bureau Co., Ltd. Key Technology Project (0877002018030101SRJS 00002); Guangdong Provincial Science and Technology Program (2017B010117008); Guangzhou Science and Technology Program (201806010106, 201902010033); the Guangdong Innovative and Entrepreneurial Research Team Program (2016ZT06D336); the Southern Marine Science and Engineering Guangdong Laboratory (Guangzhou) (GML2019ZD0301); the GDAS's Project of Science and Technology Development (2016GDASRC-0211, 2018GDASCX-0403, 2019GDASYL-0301001, 2017GDASCX-0101, 2018GDASCX-0101).

References

1. Bin, F.: Shallow Sea Bottom Topography Mapping by SAR. Ocean University of China, Qingdao (2005)
2. Cao, B.: A Study of Remotely-Sensed Data Processing in Bathymetry. Information Engineering University, Zhenzhou (2017)
3. Wang, Y., Dong, W., Zhang, P.: Advances in water depth visible light sensing methods. Marine Notif. **26**(5), 92–101 (2007)
4. Ma, Y., Zhang, J., Zhang, J., Zhang, Z., Wang, J.: Progress in shallow water depth mapping from optical remote sensing. Adv. Marine Sci. **36**(3), 331–351 (2018)
5. Huang, W., Wu, D., Yang, Y., et al.: Shallow sea multi-spectral remote sensing water depth inversion technique. J. Marine Technol. **32**(2), 43–46 (2013)
6. Bierwirth, P.N., Lee, T.J., Burne, R.V.: Shallow sea-floor reflectance and water depth derived by unmixing multispectral imagery. PE & RS **59**(3), 331–338 (1993)
7. Liu, Z., Hu, L., He, M.: Inversion of shallow water depth and optical parameters around Islands and reefs in the South China Sea by EO-1/Hypeion data. Period. Ocean Univ. China **44**(5), 101–108 (2014)
8. Tian, Z.: Research on Deep Multi/High Spectral Remote Sensing Model and Water Depth Topographic Map Production Technology in Shallow Seawater. Shandong University of Science and Technology, Qingdao (2015)
9. Shi, Y.: Ultra-spectral Remote Sensing Shallow Seawater Inversion Based on Artificial Neural Network Technology. Ocean University of China, Qingdao (2005)
10. Wang, X.: Remote Sensing Imaging Mechanism and Inversion of Typical Underwater Terrain by SAR in Shallow Sea. Zhejiang University, Zhejiang (2018)
11. Fan, K., Huang, W., He, M., et al.: Overview of remote sensing technology for shallow seawater topography by SAR. Progr. Geophys. **24**(2), 714–720 (2009)

12. Eugenio, F., Marcello, J., Martin, J.: High-resolution maps of bathymetry and benthic habitats in shallow-water environments using multispectral remote sensing imagery. IEEE Trans. Geosci. Remote Sens. **53**(7), 3539–3549 (2015)
13. Jiran, L.I., Zhang, H., Hou, P., et al.: Mapping the bathymetry of shallow coastal water using single-frame fine-resolution optical remote sensing imagery. Acta Oceanologica Sinica **35** (1), 60–66 (2016)
14. Zhao, Y.: Principles and Methods of Remote Sensing Application Analysis. Science Press, Beijing (2013)
15. Zhang, Y.: Study of fathoming method by RS technology. J. Hohai Univ. **26**(6), 68–72 (1998)
16. Ping, Z.: Mathematical model of visible light remote sensing sounding. Ocean Lake Marsh **13**(3), 225–230 (1982)
17. Ye, M., Li, R., Xu, G.: Multi-spectral water depth remote sensing methods and research progress. World Sci. Technol. Res. Dev. **29**(2), 76–79 (2007)
18. Lyzenga, D.R.: Passive remote sensing techniques for mapping water depth and bottom features. Appl. Opt. **17**(3), 379 (1978)
19. Chen, Q., Deng, R., Qin, Y., et al.: Remote sensing of water depth in Feilaixia Reservoir Area, Guangdong Province. J. Sun Yat-Sen Univ. (Nat. Sci. Ed.) **51**(1), 122–127 (2012)
20. Polcyn, F.C., Sattinger, I.J.: Water depth determinations using remote sensing techniques. Remote Sens. Environ. **II**, 13–16 (1969)
21. Tanis, F.J., Hallada, W.A.: Evaluation of landsat thematic mapper data for shallow water bathymetry. In: Proceeding of 18th International Symposium on Remote Sensing of Environment, Ann Arbor, Michigan, pp. 629–643 (1984)
22. Tanis, F.J., Byrne, H.J.: Optimization of multispectral sensors for bathymetry applications. In: Proceeding of 19th International Symposium on Remote Sensing of Environment, Ann Arbor, Michigan, pp. 865–874 (1985)
23. Wei, J., Daniel, L.C., William, C.K.: Satellite remote bathymetry: a new mechanism for modeling. Photogram. Eng. Remote Sens. **58**(5), 545–549 (1992)
24. Hang, Q., Wang, X.: Remote sensing research methods and applications of river evolution. J. Sun Yat-Sen Univ. Nat. Sci. Ed. **38**(5), 109–113 (1999)
25. Tian, S., Hong, Y., Qin, X.: Remote sensing of water depth in high-concentration salt lakes. Remote Sens. Land Resour. **18**(1), 26–30 (2006)
26. Guo, X., Qiu, Z., Shen, W., et al.: Shallow water depth inversion in Longwan port based on WorldView-2 remote sensing image. J. Marine Sci. **35**(3), 27–33 (2017)
27. Tian, Q., Wang, J., Du, X.: Remote sensing study of Jiangsu coastal water depth. J. Remote Sens. **11**(3), 373–379 (2007)
28. Zhang, D., Wang, W., Zhang, Y.: Remote sensing of water depth in the Yangtze River estuary. J. Hohai Univ.: Nat. Sci. Ed. **26**(6), 86–90 (1998)
29. Chen, M., Li, S., Kong, Q.: Satellite remote sensing water depth in the Yangtze River estuary. J. Water Resour. Water Eng. **2003**(2), 61–64 (2003)
30. John, M.P., Robert, E.S.: Water depth mapping from passive remote sensing data under a generalized ratio assumption. Appl. Opt. **22**(8), 1134–1135 (1983)
31. Clark, R.K., Fay, T.H., Walker, C.L.: Bathymetry calculations with Landsat 4 TM imagery under a generalized ratio assumption. Appl. Opt. **26**(19), 4036–4038 (1987)
32. Di, K., Qian, D., Wei, C., et al.: Shallow water depth extraction and chart production from TM image in Nansha Islands and nearby sea area. Remote Sensing of Land and Resources **41**(3), 59–64 (1999)
33. Xu, D.: Remote sensing study on water depth distribution in the Yellow River estuary. Remote Sens. Technol. Appl. **7**(3), 17–23 (1992)

34. Stumpf, R.P., Holderied, K., Sinclair, M.: Determination of water depth with high-resolution satellite imagery over variable bottom types. Limnol. Oceanogr. **48**(1), 547–556 (2003)
35. Guo, X., Qiu, Z., Tan, Q., et al.: Shallow water depth extraction from OLI remote sensing image in Basuo port. Hydrogr. Surv. Charting **37**(6), 54–57 (2017)
36. Chen, A., Ma, Y., Zhang, J.: Applicability of water depth passive optical remote sensing inversion model. Marine Environ. Sci. **37**(6), 953–960 (2018)
37. Lyzenga, D.R.: Remote sensing of bottom reflectance and water attenuation parameters in shallow water using aircraft and Landsat data. Int. J. Remote Sens. **2**(1), 71–82 (1981)
38. Li, X., Xu, Y., Wang, Y., et al.: Establishment and application of BP artificial neural network adaptive learning algorithm. Syst. Eng. Theory Pract. **24**(5), 1–8 (2004)
39. Wang, Y., Zhang, Y.: Study on remote sensing of water depth based on BP artificial neural networks. Ocean Eng. **23**(4), 33–38 (2005)
40. Cao, B., Qiu, Z., Zhu, S., et al.: Improvement of BP neural network remote sensing water depth inversion algorithm. Bull. Surv. Mapp. **2017**(02), 40–44 (2017)
41. Sandidge, J.C., Holyer, R.J.: Coastal bathymetry from hyperspectral observations of water radiance. Remote Sens. Environ. **65**(3), 341–352 (1998)
42. Lee, Z., Carder, K.L., Mobley, C.D., et al.: Hyperspectral remote sensing for shallow waters. 2. Deriving bottom depths and water properties by optimization. Appl. Opt. **38**(18), 3831–3843 (1999)
43. Lee, Z., Carder, K.L., Chen, R.F., et al.: Properties of the water column and bottom derived from airborne visible infrared imaging spectrometer (AVIRIS) data. J. Geophys. Res. Oceans **106**(C6), 11639–11651 (2001)
44. Mcintyre, M.L., Naar, D.F., Carder, K.L., et al.: Coastal bathymetry from hyperspectral remote sensing data: comparisons with high resolution multibeam bathymetry. Mar. Geophys. Res. **27**(2), 129–136 (2006)
45. Lee, Z.P., Casey, B., Arnone, R.A., et al.: Water and bottom properties of a coastal environment derived from hyperion data measured from the EO-1 spacecraft platform. J. Appl. Remote Sens. **1**(1), 011502 (2007)
46. Zhang, L., Teng, H., Meng, C., et al.: Hyperspectral remote sensing water depth detection method based on semi-analytical model. Ocean Mapp. **31**(4), 17–21 (2011)
47. Liu, Z., Zhou, Y.: Direct inversion of shallow-water bathymetry from EO-1 hyperspectral remote sensing data. Chin. Opt. Lett. **9**(6), 060102 (2011)
48. Huang, W., Fu, B., Zhou, C., et al.: Research on remote sensing method of spaceborne synthetic aperture radar in shallow seawater. In: National Remote Sensing Technology Academic Exchange Conference (2001)
49. Calkoen, C.J., Hesselmans, G.H.F.M., Wensink, G.J., et al.: The bathymetry assessment system: efficient depth mapping in shallow seas using radar images. Int. J. Remote Sens. **22**(15), 2973–2998 (2001)
50. Wensink, G.J., Hesselmans, G.H.F.M., Calkoen, C.J., et al.: The bathymetry assessment system. Oceanography **62**(97), 214–223 (1997)
51. Hennings, I., Metzner, M., Calkoen, C.J.: Island connected sea bed signatures observed by multi-frequency synthetic aperture radar. Int. J. Remote Sens. **19**(10), 1933–1951 (1998)
52. Bi, X.: SAR Detection Model for Shallow Seawater Terrain Based on Polarization Information. China University of Petroleum, Qingdao (2010)
53. Xia, C., Yuan, Y.: SAR image simulation and inversion of seabed topography in Tangguhai area. Adv. Marine Sci. **21**(4), 437–445 (2003)
54. Yang, J., Zhang, J., Meng, J.: Using SAR images to detect underwater Terrain in shallow seas of Taiwan. Chin. J. Ocean Lakes **28**(3), 636–642 (2010)
55. Li, Z., Wang, X., Yu, X., et al.: An improved method for SAR image inversion of shallow sea topography. Electron. Meas. Technol. **2012**(4), 86–89 (2012)